

A FINITE-STATE AEROELASTIC MODEL FOR ROTORCRAFT PILOT-ASSISTED-OSCILLATIONS ANALYSIS

Jacopo Serafini, Marco Molica Colella and Massimo Gennaretti
University Roma Tre, Dept. of Mechanical and Industrial Engineering,
Via della Vasca Navale 79 - 00146 Rome, Italy

Abstract

Rotorcraft-pilot couplings denote interactions between pilot and helicopter (tiltrotors) that may become adverse. They are usually divided into two main classes of phenomena: that including Pilot Induced Oscillations (PIO) phenomena driven by flight dynamics and behavioural processes, and the one conventionally named Pilot Assisted Oscillations (PAO) which is caused by unintentional actions of pilot on controls, due to his involuntary reaction to seat vibrations. The aim of this paper is the development of mathematical helicopter models suited for analysis of PAO phenomena. PAO are strictly related to the structural dynamics of the fuselage and to servoelectricity, but a crucial role is played by main rotor aeroelasticity. This paper presents a finite-state model of main rotor aeroelastic behavior that may conveniently be applied for PAO stability and response analysis, as well as for control applications aimed at PAO alleviation. It is validated, and its sensitivity to the aerodynamic modeling used within the aeroelastic operator is examined. Further, it is coupled with fuselage dynamics, servo-elastic and pilot models in order to carry out a numerical investigation concerning the stability analysis of vertical bouncing, which is a type of PAO instability which might be caused by the coupling, through the pilot, of vertical acceleration of pilot seat with collective control stick.

1. INTRODUCTION

Aircraft/Rotorcraft Pilot Coupling (A/RPC) denotes a really broad and wide category of phenomena. Despite the final effects of A/RPC events are similar, ranging from high discomfort to catastrophic crash, the causes can be utterly different. In the last years, the helicopter scientific community has finally focused the attention on these very complex events, following the path of earlier interests in the fixed-wing aircraft field. At present, the European project *ARISTOTEL (2010-2013)* is active with the aim of predicting the proneness of modern aircraft and rotorcraft to A/RPC, and identifying suitable guidelines to design of next generation aircraft such to avoid adverse A/RPC.¹ In the past, both analysis and recognition of a RPC event have often been very

difficult tasks. Not only due to the effective challenge to reconstruct an accident scene, but also because of the lack of awareness of the possible witnesses, even when highly trained. Indeed, RPC events are always associated to a mismatch between pilot's mental model of vehicle dynamics and the actual one, up to a complete unawareness of the catastrophic events going on. From a physical point of view, their analysis is very complicated as it involves structural dynamics, rigid body dynamics, servoelectricity, automatic flight control system and, of course, biodynamic and piloting. In the last years, effort was made by the research community to distinguish RPC events into different classes. The most functional classification is based on the frequency content of the dynamics involved, for which Rigid

Body RPCs (frequency range 0 – 2Hz) are separated from Aeroelastic RPCs (frequency range 2 – 8Hz). In the first class of phenomena, also named PIO (Pilot Induced Oscillation), the pilot response is dominated by a behavioral process (mental mismatch, as said above), whereas in the second one, the pilot acts like an unconscious link between seat motion and controls, thus acting like a mechanical impedance. Differently from the fixed-wing world, where almost the total amount of APC events is characterized by PIOs, the available statistics clearly shows that PAOs are a very relevant portion of RPC accidents, thus requiring greater attention. At the frequency range involved in PAO, the pilot unaware actions couple, among others, with blades dynamics, airframe flexibility and servos, thus requiring more complex tools for effective computational simulations.

Here, developments of a comprehensive tool for RPC investigations are presented and applied. It is the result of the last years efforts of the authors in this field, particularly focused on PAO analysis.²⁻⁴ It includes fuselage, servoelasticity and pilot modeling, as well as main rotor modeling that has been proven to play a crucial role in PAO phenomena. The novelty presented in this paper consists of the introduction of a finite state modeling of the aeroelastic behavior of the main rotor. This main rotor aeroelastic operator is developed following an approach similar to that presented and validated in the past by some of the authors for rotor aerodynamics.⁵ It yields a constant-coefficient, linear, differential form relating hub motion dofs and blade controls to the corresponding loads transmitted to the fuselage, with the by-product of the introduction of a finite number of additional states related to dynamics of wake vorticity and blades (indeed, blade dofs do not appear explicitly in this model). Therefore, it allows the identification of a linearized, time-invariant (LTI), state-space form of the rotorcraft mathematical model, suited for PAO stability analysis and aeroservoelastic applications. This approach requires the prediction of a set of harmonic perturbation responses by an aeroelastic solver. The accuracy of this solver characterizes the one of the identified finite-state operator. In particular, depending on the aerodynamic formulation applied, it might take into account

the mutual aerodynamic influences between rotor blades, fuselage and tail-rotor, hence yielding a detailed helicopter model.

For the work presented here, the main rotor aeroelastic model is obtained by coupling a beam-like, nonlinear, bending-torsion model for the structural dynamics of nonuniform, twisted blades^{6,7} with an aerodynamic solver based on a Boundary Element Method formulation for potential flows,⁸ which is fully three-dimensional, and may include complex effects like wake roll-up, wake-blade or wake-fuselage impingements. The complete helicopter model is determined by coupling the main rotor model with fuselage dynamics as given by the superposition of rigid-body motion and deformation motion described through a modal approach with mass, damping and stiffness matrices obtained through a FEM analysis.² The main rotor also interacts with the servoelastic model, described by a second order transfer function relating the command stick angle to the blade pitch control angle. For PAO analyses, a pilot model that concerns only biodynamic response is introduced in the loop. It is described in terms of a transfer function between pilot seat motion and command stick displacement, with coefficients depending on the pilot size/weight.

The numerical investigation has three main objectives: firstly, the finite-state, aeroelastic modeling of the main rotor is validated by comparison with direct, time-marching predictions from the complete formulation; secondly, the effects of different aerodynamic modeling on aeroelastic responses are examined by comparing the corresponding transfer functions that relate hub loads to hub motion and pilot controls; finally, the LTI model of the piloted, flexible-airframe helicopter is applied, showing its capability to assess the proneness to adverse PAO phenomena. In particular, the problem known as "vertical bouncing" is investigated. It is an instability which might be caused by the coupling, through the pilot, of vertical acceleration of pilot seat with collective control stick.^{9,2}

2. RPC PHENOMENOLOGY

As outlined above, RPCs include a wide class of phenomena related to structural dynamics, rigid body dynamics, servoelasticity, automatic flight

control system and, of course biodynamics and piloting.

During the last decades, they have been classified into two main groups, Rigid Body RPC and Aeroelastic RPC, on the basis of the prevalent dynamics involved and the consequent range of frequency of interest (0 – 2Hz and 2 – 8Hz, respectively). This distinction is similarly applicable to the type of feedback exerted by the pilot: in the first case, his response is dominated by behavioural processes, in the second one the pilot is an inadvertent link between seat motion and controls, acting *de facto* like a mechanical impedance. Figure 1 shows a typical spectrum of phenomena and helicopter characteristics involved in RPC occurrence.

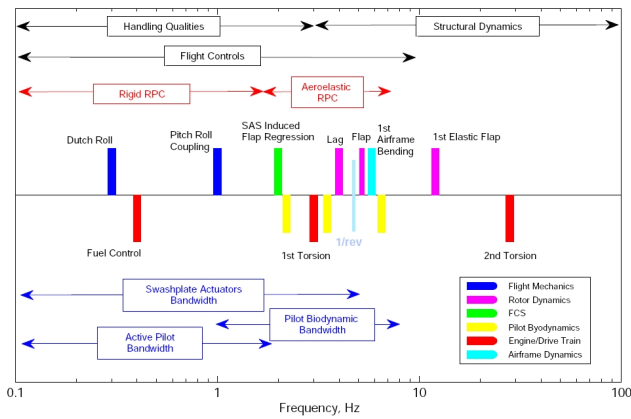


Figure 1. Spectrum of phenomena involved in RPC.

Finally, it is worth noting that another usual way to classify RPC phenomena considers the properties of the system with respect to the linearity of the phenomena and the triggers of instabilities. Category I comprises those phenomena that may be described through linearized systems, Category II comprises those phenomena where non-linear effects are relevant (like, for instance, saturation of control actuation), while in Category III instabilities arising in the presence of some triggers, like malfunctioning or gust, fall.

3. MAIN ROTOR FINITE-STATE AEROELASTIC MODEL

In order to derive the state-space representation of piloted helicopter dynamics, the aeroelastic behavior of the main rotor is expressed in terms

of a finite-state, LTI operator. For a given steady flight condition, it relates forces and moments produced by the rotor at the main rotor hub attachment point, \mathbf{f}_{MR} , to the components of motion at that point (displacements and rotations given by combination of rigid-body motion and airframe deformation), \mathbf{x}_{MR} , and to the main rotor controls, $\mathbf{u}_{MR} = \{\theta_0 \theta_{1c} \theta_{1s}\}$. Since the main rotor aeroelastic behavior is intrinsically periodic and nonlinear, and because of time-delayed contributions introduced by unsteady aerodynamics through wake vorticity effects (and compressibility effect, if taken into account), the finite-state, LTI aeroelastic operator is identified by a dual-step process: first, the transfer functions relating hub loads to hub motion and controls are identified, starting from aeroelastic responses predicted by a time marching solver, such that the following expression holds

$$(1) \tilde{\mathbf{f}}_{MR} = \mathbf{H}_x(i\omega) \tilde{\mathbf{x}}_{MR} + \mathbf{H}_u(i\omega) \tilde{\mathbf{u}}_{MR}$$

and then, the transfer function matrices, \mathbf{H}_x and \mathbf{H}_u , are approximated by rational-matrix forms, in order to get a finite-state representation of the rotor loads transmitted to the fuselage (indeed, unsteady aerodynamics contribution makes transfer functions of transcendental nature, thus giving rise to an infinite-dimension state-space problem). Note that rotor blades dofs do not appear explicitly in this description: their effects are considered through the states related to the poles of the rational-matrix approximation of the aeroelastic operator (see later, Subsection 3.3).

In the following, the procedure for identification of the LTI operator and the rotor aeroelastic solver it is based on are outlined.

3.1 The Aeroelastic Solver

A nonlinear, bending-torsion, beam-like model valid for straight, slender, homogeneous, isotropic, nonuniform, twisted blades undergoing moderate displacements is applied to represent the structural dynamics of main rotor.^{6,7} The radial displacement is eliminated from the set of equations by solving it in terms of local tension, and thus the resulting structural operator consists of a set of coupled nonlinear differential equations governing the bending of the elastic axis (lead-lag and flap deflections) and the rotation of the cross

sections (blade torsion). If present, the effects of blade pre-cone angle, hinge offset, torque offset and mass offset are included in the model, as well as the kinematic effects due to hub motion.

The aeroelastic formulation is determined by coupling this structural dynamics model with a model for the description of the distributed aerodynamic loads. In this work, the rotor aerodynamic loads are simulated either through a sectional model combined with wake-inflow corrections to account for the three-dimensional trailing vortices effects,¹⁰ or introducing a Boundary Element Method (BEM) solver for free-wake, potential flows. The BEM computational tool considered is based on a velocity-potential, boundary integral equation formulation suited for the prediction of aerodynamics of rotors, that is applicable to a wide range of flight configurations, including those with complex blade-vortex interactions onset.^{8,11} The blade pressure distribution is determined by the Bernoulli theorem and the distributed forces and torque moment are obtained by integration over cross-section profile contours.

The Galerkin approach is applied for the spatial integration of the resulting aeroelastic integro-differential formulation while, time responses are computed through a time marching, Newmark- β numerical scheme. Once the rotor aeroelastic response is computed, forces and moments at the hub attachment point are evaluated through combination of the corresponding aerodynamic and inertial blade loads.

3.2 The Aeroelastic Transfer-Function Matrices

For a helicopter rotor in arbitrary steady flight, the aeroelastic model described above is intrinsically nonlinear, with periodic coefficients. As a consequence, even a single-harmonic, small perturbation of rotor controls or hub motion yields multi-harmonic loads at the hub attachment point, and this behavior cannot be modeled by means of a LTI operator. However, akin to what widely applied in multiblade aeroelastic analyses of isolated helicopter rotors, for the present problem an accurate linearized modeling can be pursued on the base of a time-invariant approximation, in that involving I/O quantities defined in the nonrotating frame.

Following the approach recently presented regarding the finite-state modeling of aerodynamics of rotors in arbitrary steady flight,^{17,5} the first step to determine the main rotor LTI aeroelastic model consists of the identification of the transfer function matrices in Eq. (1) in the way herein described: (i) the time marching solution of the complete aeroelastic formulation is applied to evaluate the perturbation loads at the hub attachment point due to single-harmonic small oscillations of each variable appearing in \mathbf{x}_{MR} and \mathbf{u}_{MR} ; (ii) the harmonic component of the responses that has the same frequency of the input is extracted and the corresponding complex value of the frequency-response functions is determined; (iii) the process is repeated for a discrete number of frequencies within an appropriate range, so as to get an adequate sampling of the frequency-response functions appearing within \mathbf{H}_x and \mathbf{H}_u . Note that, extracting from the perturbation output only the contribution having the same harmonic of the input implies that a linearized, constant-coefficient approximation of the operators yielding \mathbf{f}_{MR} from \mathbf{x}_{MR} and \mathbf{u}_{MR} is pursued (indeed, in nonlinear and/or periodic-coefficient relations a single-harmonic input yields outputs that are multi-harmonic).⁵

Further, it is worth mentioning that the harmonic components are obtained through a discrete Fourier transform algorithm, taking care of the following issues:^{5,12} (i) the period examined starts after that the aeroelastic transient response to the perturbation is finished; (ii) the period examined has to be an integer multiple of the period of the input harmonic; (iii) almost periodic loads might arise because of the intrinsic periodicity of the aeroelastic system, and hence the leakage avoidance is assured if, in addition, the period examined is long enough.

Finally, note that the approach described is applicable under condition of aeroelastic stability of the isolated rotor in the steady flight configuration for which the transfer-function matrices are identified.

3.3 Rational-Matrix Approximation and Finite-State Representation

The final step in the process of identification of a

finite-state representation of the aeroelastic operator consists of deriving rational forms (with a finite number of poles) that have the best fit to the sampled transfer functions, followed by transformation into time domain.

Specifically, from the application of a least-square procedure assuring the stability of the identified poles, the overall transfer-function matrix $\mathbf{H} = \{\mathbf{H}_x \mathbf{H}_u\}$ obtained from the assembly of the matrices \mathbf{H}_x and \mathbf{H}_u , is approximated as¹³

$$(2) \quad \mathbf{H}(s) \approx s^2 \mathbf{A}_2 + s \mathbf{A}_1 + \mathbf{A}_0 + \mathbf{C} [s \mathbf{I} - \mathbf{A}]^{-1} \mathbf{B}$$

where $\mathbf{A}_2, \mathbf{A}_1, \mathbf{A}_0, \mathbf{A}, \mathbf{B}$ and \mathbf{C} are real, fully populated matrices, while s denotes the Laplace-domain variable. Techniques of this type are frequently used for the reduced-order representation of fixed wings aerodynamic loads,¹⁴ and have already been applied for modeling aerodynamics of rotors in axial flow.¹⁵

Finally, for \mathbf{x} denoting the vector collecting hub motion and rotor control variables, *i.e.*, such that $\mathbf{x}^T = \{\mathbf{x}_{MR}^T \mathbf{u}_{MR}^T\}$, combining Eq. (2) with Eq. (1) and transforming into time domain yield the following finite-state representation of the loads transmitted to the fuselage by the main rotor

$$(3) \quad \begin{aligned} \dot{\mathbf{f}}_{MR}(t) &= \mathbf{A}_2 \ddot{\mathbf{x}} + \mathbf{A}_1 \dot{\mathbf{x}} + \mathbf{A}_0 \mathbf{x} + \mathbf{C} \mathbf{r} \\ \dot{\mathbf{r}} &= \mathbf{A} \mathbf{r} + \mathbf{B} \mathbf{x} \end{aligned}$$

where \mathbf{r} is the vector that collects the additional states associated to the poles included in the approximating rational matrix. These additional states replace and take into account the dynamics of the rotor blades dofs which, in this approach, only implicitly affects the aeroelastic transfer functions. At the same time, they are also a consequence of the flow-memory (delay) effects due to unsteady wake vorticity, that are responsible for the transcendental nature of aerodynamics transfer functions.¹⁶

4. AERO-SERVO-ELASTIC HELICOPTER MODEL

Flexible fuselage dynamics, control chain dynamics and pilot passive behavioral dynamics participate together with main rotor aeroelasticity to the assembly of the helicopter LTI comprehensive simulation model suited for PAO analysis.

The main rotor model interacts both with fuselage dynamics through hub loads and motion and with the control-chain servoelastic model which yields the rotor blade commands, while the pilot behavioral model receives the seat motion as input and supplies the collective stick displacement to the control-chain servoelastic model (see Fig. 2). Each component of the helicopter model is developed with the necessary level of accuracy, introducing the optimal number of degrees of freedom, with a clear definition of I/O variables, so as to allow it to be changed easily.

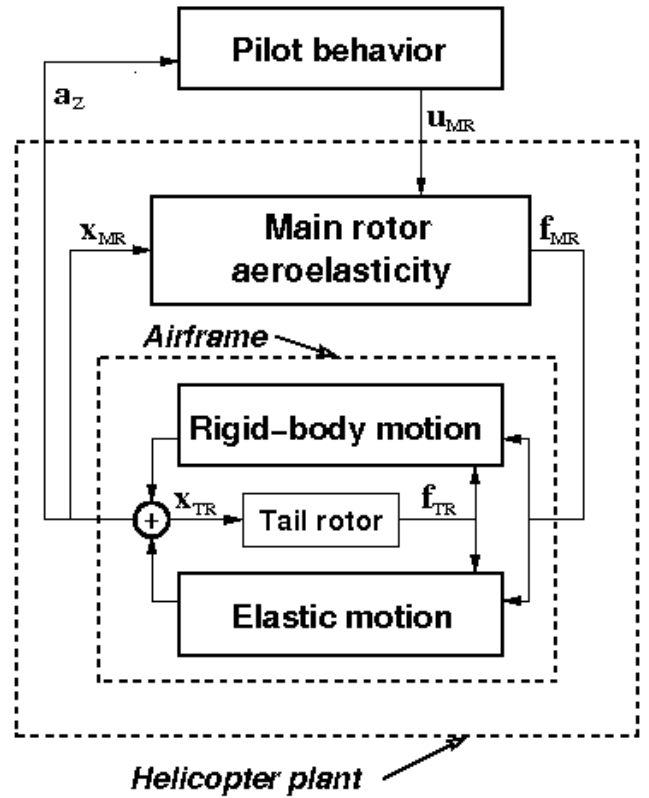


Figure 2. Block diagram of RPC.

4.1 Fuselage model

In RPC insurgency, a crucial role is played by fuselage dynamics. In particular, as demonstrated by past investigations, pilot seat vibrations due to fuselage elastic dynamics are of fundamental importance in PAO phenomena.^{1,2} The LTI fuselage model considered here consists of combination of small-disturbance, rigid-body motion equations with fuselage elastic-deformation equations.

The rigid-body equations derive from the stan-

standard six degrees of freedom model enriched by Euler angles kinematics for the definition of vehicle orientation, linearized about an arbitrary steady flight condition.¹⁸ Main forcing terms to these equations are the main rotor hub loads, but contributions from tail rotor and fuselage aerodynamics are taken into account, as well (see Fig. 2).

Fuselage elastic dynamics is expressed through the following modal approach

$$(4) \quad M_\xi \ddot{\xi} + C_\xi \dot{\xi} + K_\xi \xi = \mathbf{f}_\xi$$

where ξ is the vector collecting the modal amplitudes (elastic degrees of freedom), M_ξ , C_ξ , K_ξ are mass, damping and stiffness matrices, whereas \mathbf{f}_ξ is the vector of the generalized forces. This model is identified through a FEM analysis dedicated to the evaluation of free-vibration modes of the unconstrained structure. Indeed, this is a convenient approach, in that the resulting elastic modes are such that rigid-body motion equations and elastic dynamics equations are coupled only through the forcing terms (see Fig. 2).² The forcing terms in Eq. (4) are obtained by projecting main rotor and tail rotor loads onto the modal shapes derived from the eigenvectors given by FEM analysis.

4.2 Servoelastic control-chain model

The control chain regarding actuators of main rotor collective pitch command is modeled by the following second-order differential form relating collective stick rotation, α , to collective pitch of the blade θ_0

$$(5) \quad \ddot{\theta}_0 + 2D\omega_\theta \dot{\theta}_0 + \omega_\theta^2 \theta_0 - \alpha = 0$$

where ω_θ is the equivalent frequency, and D denotes damping. Cyclic pitch controls and tail rotor pitch may be related to lateral command motion and pedals through similar differential forms. However, it has been proven that they have very small influence on the vertical bouncing PAO phenomena that will be examined in the numerical investigation.²

4.3 Pilot model

Indeed, pilot model is an essential feature of a RPC prediction tool. For the frequency range of interest in PAO analysis (higher than 2Hz),

the behaviour of the pilot is dominated by biodynamic phenomena (excited by seat vibrations), making voluntary piloting modeling unnecessary.

First helicopter pilot passive (involuntary behavior) models have been introduced by Mayo,⁹ who expressed them in terms of transfer functions between vertical seat acceleration (input), a_z , and vertical acceleration of the pilot hand (output), a_0 (see Fig. 2). Specifically, exploiting the results of a dedicated experimental campaign, the following models for ectomorphic (lighter) and mesomorphic (heavier) pilots, respectively, have been identified⁹

$$(6) \quad H_{ecto} = G \frac{5.19s + 452.3}{s^2 + 13.7s + 452.3}$$

$$(7) \quad H_{meso} = G \frac{4.02s + 555.4}{s^2 + 13.31s + 555.4}$$

where G denotes the gain of the transfer functions. These two transfer functions (depicted in Fig. 3) present two poles and one zero, with coefficients dependent on the position of stick and arm.⁹ However, an appropriate definition of the gain value may approximate this effect.

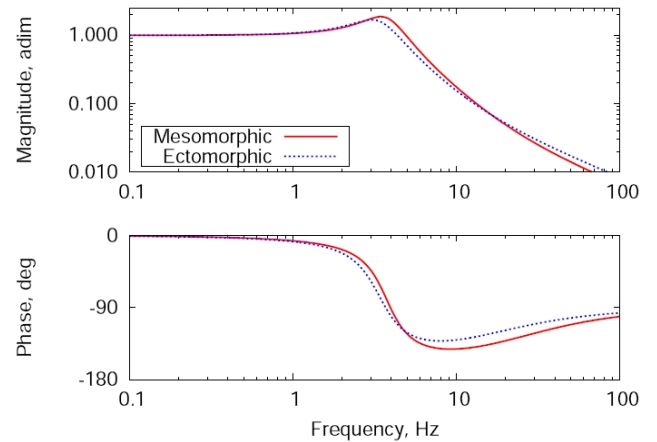


Figure 3. Mayo's transfer functions between seat and control stick accelerations.

The hand acceleration is related to the collective stick rotation as follows

$$(8) \quad r_{st} \tilde{\alpha} s^2 \simeq \tilde{a}_0 - \tilde{a}_z$$

with r_{st} denoting the length of the collective stick, and seat acceleration a_z given by combination of the rigid-body motion and elastic deformation of the fuselage.

5. NUMERICAL RESULTS

The helicopter configuration examined in the numerical investigation is representative of a light-weight helicopter, with hingeless rotor design, closely related to the Bo-105. The main rotor has four blades, with radius, $R = 4.94\text{m}$, constant chord, $c = 0.395\text{m}$, linear twist of -8° and nominal rotational speed $\Omega = 44.4\text{rad/s}$. The airframe is described by the 3 natural modes of vibration having eigenfrequencies of about 5.5Hz, 7.5Hz and 11.5Hz.² The first mode is dominated by bending of the airframe about the pitch axis, with out of phase relative vertical motion between the main rotor attachment and the cabin floor, that may cause significant interaction between helicopter vertical oscillation and pilot inadvertent reaction. The elastic behavior of the rotor blades within the time-marching, aeroelastic rotor solver has been modeled through one flap mode, two lag modes and one torsion mode. In the following, results concerning the validation of the main rotor LTI, finite-state aeroelastic model and those regarding PAO stability analysis are presented and discussed.

5.1 Validation of LTI, finite state, aeroelastic rotor model

First, for a hovering flight configuration, the effect of the aerodynamic model on the LTI main rotor aeroelastic operator identified through the approach presented above is examined. Specifically, Figs. 4 and 5 show the comparison between transfer functions identified through the aeroelastic solver based on sectional aerodynamic theory and those given by the aeroelastic predictions derived from application of the BEM solver. Figure 4 illustrates the transfer function between the axial force and the axial motion of the hub, while Fig. 5 concerns the transfer function between the roll moment and the lateral cyclic pitch control. In both cases, the two solutions have a similar trend with respect to frequency: this is expected in that rotor blade elastic properties have a strong influence on poles and zeroes of the aeroelastic response function. Anyway, some discrepancies arise that may locally imply not negligible differences in amplitude and phase of response.

Next, the accuracy of the rational matrix approx-

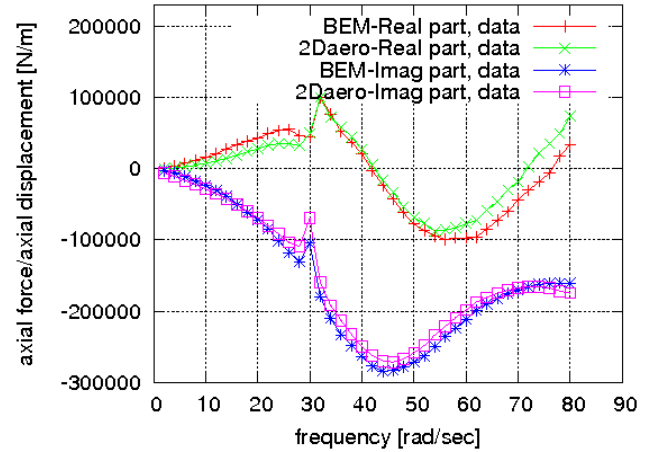


Figure 4. Transfer function between axial force and hub axial displacement. BEM vs Sectional aerodynamics, hovering flight.

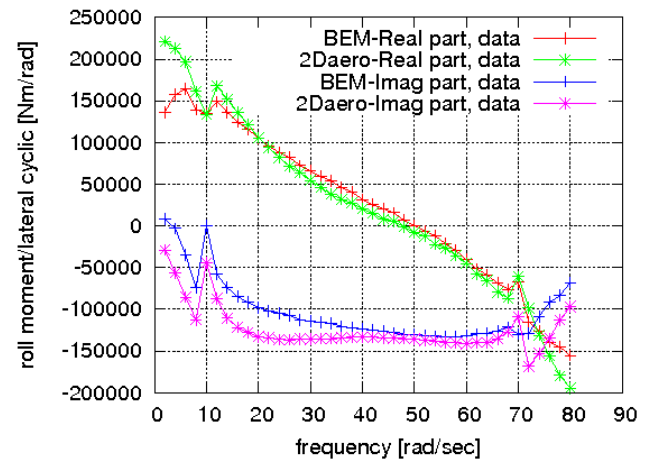


Figure 5. Transfer function between roll moment and lateral cyclic pitch. BEM vs Sectional aerodynamics, hovering flight.

imation (RMA) applied in the process of identification of the finite-state main rotor aeroelastic model is assessed. To this purpose, Figs. 6 and 7 present the rational matrix approximation of transfer functions from aeroelastic solutions based on BEM aerodynamics, while Fig. 8 shows the rational matrix approximation of a transfer function given by sectional aerodynamics. Specifically, Figs. 6 and 7 concern axial force vs hub axial displacement and yaw moment vs longitudinal cyclic pitch in hovering conditions, respectively, whereas Fig. 8 regards axial force vs collective pitch for a forward flight condition with advance ratio, $\mu = 0.3$. These figures demonstrate the high level of accuracy of

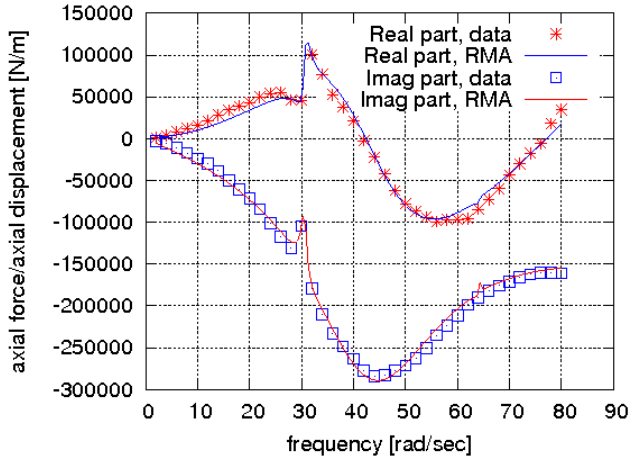


Figure 6. Transfer function between axial force and hub axial displacement. Sampled BEM solution vs RMA, hovering flight.

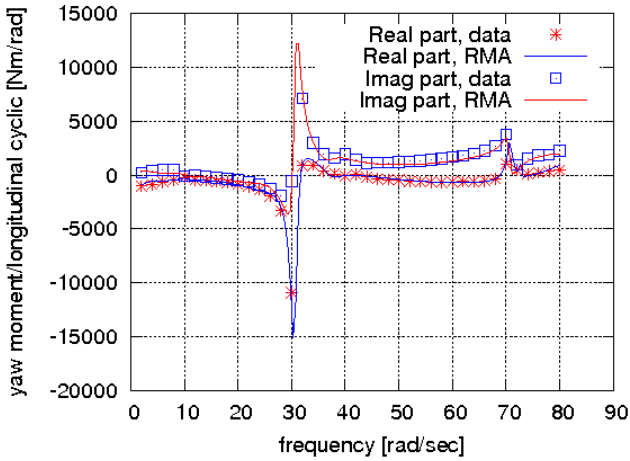


Figure 7. Transfer function between yaw moment and longitudinal cyclic pitch. Sampled BEM solution vs RMA, hovering flight.

the approximation of the main rotor aeroelastic transfer functions that may be obtained through the rational matrix form presented above. It guarantees (with no reference to the constant-coefficient approximation that is discussed soon later) a very good level of accuracy for the corresponding finite-state representation of the LTI aeroelastic rotor model.

The quality of the differential, LTI, finite-state model in describing the rotor-hub perturbative forces and moments is assessed by comparison with the results given by the non-linear, time marching (NLTM) solution of the complete aeroelastic model. They are generated by the following arbitrary perturbation, θ_{com} , of one of the

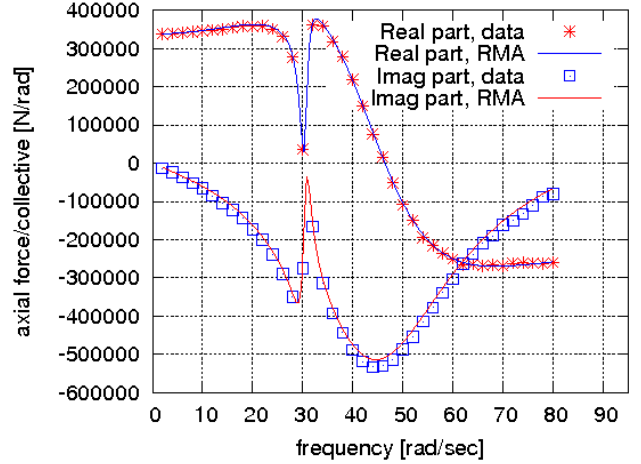


Figure 8. Transfer function between axial force and collective pitch. Sampled sectional aerodynamics solution vs RMA, advancing flight.

command inputs

$$(9) \quad \theta_{com} = A \sin(\omega t) \cos(2\omega t) e^{(-\alpha t)}$$

with $A = 0.01$, $\omega = 0.3\Omega$ and $\alpha = 0.004\Omega$. Figure 9 shows the thrust generated by a perturbation of the collective pitch angle ($\theta_0 \equiv \theta_{com}$) during the hovering flight condition. As it can be seen, the LTI, finite-state approximation is very effective in reproducing the periodic aeroelastic system. However, in this case significant time-periodic terms in the aeroelastic system are absent and the time-invariance approximation is active only on some contributions from the small cyclic pitch angles that are present in the trim control setting. Significant time-periodic terms are present in the forward-flight condition that is examined in Fig. 10, where the rolling moment due to the perturbation to the lateral cyclic pitch command is depicted. Even in this case ($\mu = 0.3$), although (as expected) more evident differences are present, these remain very small and the LTI, finite-state model demonstrates to be able to yield a very accurate representation of the aeroelastic loads.

5.2 PAO analysis

Finally, the LTI model of the complete helicopter is applied with and without inclusion of pilot in the loop, for the stability analysis. This is one of the most significant application of the proposed rotor aeroelastic model, because of the relatively low amount of rotor states it requires

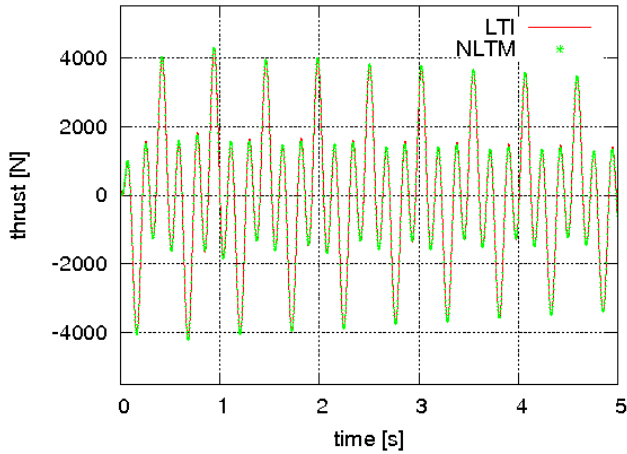


Figure 9. Thrust. LTI vs NLTM

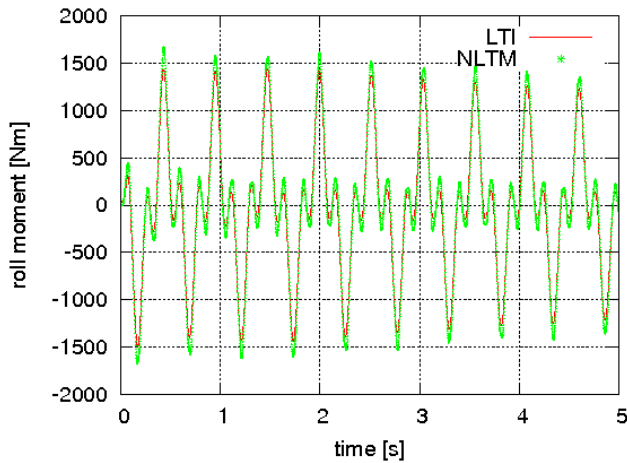


Figure 10. Rolling moment. LTI vs NLTM

(about forty in the proposed case). In particular, here the only pilot feedback present is through the collective pitch control, which is the control mainly involved in vertical bouncing phenomena.

Figures 11 and 12 present the stability behavior of the helicopter for the hovering flight condition, as evaluated using sectional rotor aerodynamics and BEM aerodynamics, respectively. The two rotor aerodynamic models yield some significant differences in helicopter dynamics prediction, in particular in terms of the influence on the elastic airframe dynamics, which play a prominent role in PAO insurgency.

Figure 13 shows that the forward flight condition seems to be more prone to PAO insurgency, although unstable PAO is not yet occurring, even in this case.

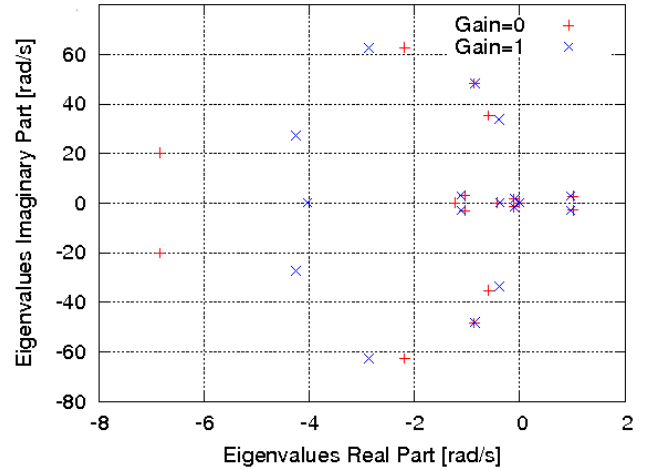


Figure 11. Helicopter dynamics root locus, with and without pilot in the loop. Hovering condition, sectional aerodynamics.

6. CONCLUDING REMARKS

In this paper a LTI piloted, helicopter model suited for RPC/PAO analyses has been presented and applied. It is obtained as an assembly of LTI models for main rotor aeroelasticity, fuselage dynamics, control-chain dynamics and pilot inadvertent (passive) behavior. The LTI main rotor contribution is obtained through an original approach that yields a finite-state model relating hub motion and pilot controls to the loads transmitted to the fuselage. The rotor blades degrees of freedom do not appear explicitly in the model, but affect the transfer functions which are identified through a time marching aeroelastic solver including them. The numerical investigation has demonstrated the capability of the rational matrix approach applied to reproduce with an excellent level of accuracy the identified transfer functions of the time-invariant approximated operator and, more important, has shown that, for an arbitrary pilot control input, the main rotor loads predicted by the LTI finite-state model are in very good agreement with those given directly by the time-marching solver. This proves that both time-invariance and finite-state approximations introduced in the aeroelastic model are acceptable and yield a formulation that can be conveniently applied for RPC/PAO aeroservoelastic purposes (specifically, for stability analysis and control-law identification). Furthermore, the reduced number of states involved and hence the

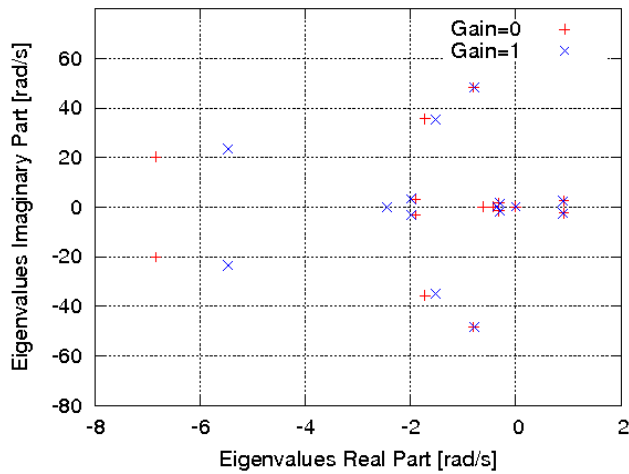


Figure 12. Helicopter dynamics root locus, with and without pilot in the loop. Hovering condition, BEM aerodynamics.

computational efficiency of this approach make it a promising tool for real-time predictions of helicopter dynamics. Main rotor transfer functions obtained using a sectional aerodynamic theory in the time-marching aeroelastic tool and those given by application of a three-dimensional, BEM aerodynamic solver have been compared. Although the zeroes and poles that characterize the response are very similar (as expected, in that closely related to the structural properties of the rotor blades), not-negligible differences have been observed, thus highlighting the important role played by aerodynamic modeling also in the kind of applications examined here. Applications to PAO stability analysis have confirmed the validity of the proposed approach. The influence of pilot passive behavior on the stability of the helicopter has been assessed for hovering and forward flight condition, showing that the latter is more critical in terms of unstable PAO insurgency. The influence of rotor aerodynamic modeling on helicopter PAO predictions has been examined, noting that it significantly affects the elastic airframe dynamics (which has an important role in PAO phenomena).

ACKNOWLEDGEMENTS

The research leading to these results has received funding from the European Community's Seventh Framework Programme (FP7/2007-2013) under grant agreement N. 266073.

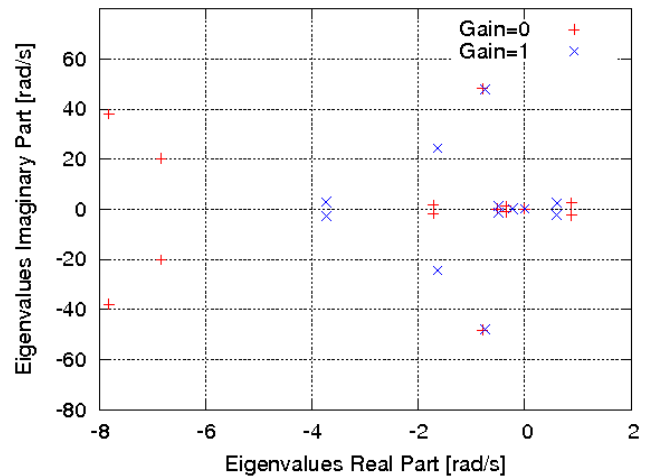


Figure 13. Helicopter dynamics root locus, with and without pilot in the loop. Forward flight condition, sectional aerodynamics.

REFERENCES

- [1] M.D. Pavel, J. Malecki, B. Dang Vu, P. Masarati, M. Gennaretti, M. Jump, M. Jones, H. Smaili, A. Ionita, L. Zaicek, "Present and Future Trends in Rotorcraft Pilot Couplings (RPCs)-A Retrospective Survey of Recent Research Activities within the European project ARISTOTEL," 37th European Rotorcraft Forum, Gallarate, Italy, Sept. 2011.
- [2] J. Serafini, M. Gennaretti, P. Masarati, G. Quaranta, O. Dieterich, "Aeroelastic and Biodynamic Modelling for Stability Analysis of Rotorcraft-Pilot Coupling Phenomena," 34th European Rotorcraft Forum, Liverpool, UK, Sept. 2008.
- [3] J. Serafini, L. Greco, M. Gennaretti, "Prediction of Rotorcraft-Pilot Coupling Phenomena Through Reduced-Order Aerodynamic Model," International Forum on Aeroelasticity and Structural Dynamics, Seattle, Washington, June, 2009.
- [4] P. Masarati, G. Quaranta, M. Gennaretti, J. Serafini, "An Investigation of Aeroelastic Rotorcraft-Pilot Interaction," 37th European Rotorcraft Forum, Gallarate, Italy, Sept. 2011.
- [5] M. Gennaretti, D. Muro, "Multiblade Reduced-Order Aerodynamics for State-Space

- Aeroelastic Modeling of Rotors," *J. of Aircraft*, Vol. 49, No. 2, pp. 495-502, 2012.
- [6] D.H. Hodges, E.H. Dowell, "Nonlinear Equation for the Elastic Bending and Torsion of Twisted nonuniform Rotor Blades," NASA TN D-7818, 1974.
- [7] M. Gennaretti, M. Molica Colella, G. Bernardini, "Prediction of Tiltrotor Vibratory Loads with Inclusion of Wing-Proprotor Aerodynamic Interaction," *J. of Aircraft*, Vol. 47, No. 1, pp. 71-79, 2010.
- [8] M. Gennaretti, G. Bernardini, "Novel Boundary Integral Formulation for Blade-Vortex Interaction Aerodynamics of Helicopter Rotors," *AIAA Journal*, Vol. 45, No. 6, 2007, pp. 1169-1176.
- [9] J. Mayo, "The Involuntary Participation of a Human Pilot in a Helicopter Collective Control Loop," 15th European Rotorcraft Forum, Amsterdam, The Netherlands, Sept. 1989.
- [10] M. Gennaretti, G. Bernardini, 'Aeroacousto-Elastic Modeling for Response Analysis of Helicopter Rotors,' in: G. Buttazzo and A. Frediani (eds.), *Variational Analysis and Aerospace Engineering: Mathematical Challenges for Aerospace Design*, pp. 7-50, Springer Science+Business Media, LLC 2012, New York, 2012.
- [11] G. Bernardini, J. Serafini, S. Ianniello, M. Gennaretti, "Assessment of Computational Models for the Effect of Aeroelasticity on BVI Noise Prediction," *Int'l J. of Aeroacoustics*, Vol. 6, No. 3, pp. 199-222, 2007.
- [12] D. Muro, M. Gennaretti, "Stability Analysis of Helicopter Rotors in Forward Flight via State-Space Aeroelastic Modeling and Correlation with Experimental Results," 37th European Rotorcraft Forum, Gallarate, Italy, Sept. 2011.
- [13] L. Morino, F. Mastroddi, R. De Troia, G.L. Ghiringhelli, P. Mantegazza, "Matrix Fraction Approach for Finite-State Aerodynamic Modeling," *AIAA Journal*, Vol. 33, No. 4, 1995, pp. 703-711.
- [14] M. Karpel, "Design for the Active Flutter Suppression and Gust Alleviation Using State-Space Aeroelastic Modeling," *Journal of Aircraft*, Vol. 19, No. 3, pp. 221-227, 1982.
- [15] M. Gennaretti, L. Greco, "A Time-Dependent Coefficient Reduced-Order Model for Unsteady Aerodynamics of Proprotors," *Journal of Aircraft*, Vol. 42, No. 1, pp. 138-147, 2005.
- [16] T. Theodorsen, "General Theory of Aerodynamic Instability and the Mechanism of Flutter," NACA Report 496, 1935.
- [17] M. Gennaretti, D. Muro, "A Multiblade Aerodynamic Reduced-Order Model for Aeroelastic Analysis of Helicopter Rotors in Forward Flight," 35th European Rotorcraft Forum, Paris, France, Sept. 2010.
- [18] G.D. Padfield, *Helicopter Flight Dynamics*, Blackwell Science Ltd, Oxford, UK, 1996.